SNOW AVALANCHE ACTIVITY MONITORING FROM SPACE: CREATING A COMPLETE AVALANCHE ACTIVITY DATASET FOR A NORWEGIAN FORECASTING REGION

Markus Eckerstorfer[1]*, Hannah Vickers[1] and Eirik Malnes[1]

[1]Norut – Northern Research Institute, Tromsø, Norway

ABSTRACT: Complete and consistent avalanche activity records, critical for avalanche forecasting, are with traditional monitoring methods not achievable in an entire avalanche forecasting region. Here we present the use of radar remote sensing, utilizing freely available Sentinel-1A SAR data in detecting avalanche debris. Through a change detection method, radar images showing a change in backscatter over time, are created, where avalanche debris become detectable as they pose a localized increase in backscatter. We have manually identified over 700 avalanche debris each during two winters (2014/15 and 2015/16) in the Norwegian avalanche forecasting region 'Tamokdalen'. This unique avalanche activity dataset allowed us to study the topographical and morphological parameters of these avalanche debris, as well as the frequency of releases in over 600 avalanche paths. For operational use of this remote detection of avalanche debris, we currently develop an automatic detection algorithm. The algorithm correctly classifies nearly 70 % of the avalanche debris identified manually, which is a promising first result. With the launch of twin satellite Sentinel-1B, every location on Earth will be imaged every six days over an area of 250x150km.

KEYWORDS: Radar remote sensing, avalanche detection, Sentinel-1A, change detection

1. INTRODUCTION

1.1 Motivation

Spatial characteristics of snow avalanche (hereafter called avalanche) activity are crucial for defining and validating the avalanche danger level. Answering the seemingly simple question: 'Where did an avalanche occur, of which size and what where the topographic and meteorological conditions favoring the release?, is for a given avalanche forecasting region with current mostly field-based monitoring approaches not possible throughout an entire winter.

In recent years, a technical revolution in avalanche activity monitoring has taken place. Remote sensing applications range from optical time lapse camera monitoring (van Herwijnen et al., 2013), to the use of LiDAR (Deems et al., 2013), seismic sensors (van Herwijnen and Schweizer, 2011) and acoustic fiber optic sensors (Prokop et al., 2014). The most recent development is satellite borne radar remote sensing of avalanches (Eckerstorfer et al., 2016). High spatial resolution radar sensors (SAR – synthetic aperture radar) have the advantage of imaging phenomena on the ground independent of cloud cover and light conditions, thus ensuring consistent all-year monitoring.

1.2 Scope of the study

In this study we wish to show that avalanche debris is detectable in SAR images and that newly operational SAR sensors allow for consistent monitoring of avalanche activity in space and time, resulting in the construction of a complete database of avalanche activity that occurred in a given avalanche forecasting region.

2. METHODS

2.1 SAR image acquisition and processing

We used imagery from the radar satellite Sentinel-1A (S1A) which was launched by ESA in 2014 as part of the environmental monitoring programme Copernicus. S1A provides in its IW (interferometric wideswath mode) free-of-charge radar images from any location on Earth every 12 days with a ground swath of 250x150km and a spatial resolution of 5x20m. However, as the satellite is in a polar orbit, numerous satellite paths overlap at higher latitudes, effectively decreasing the repetition time to 2-3 days at 70 degrees latitude. In Fig 1 we show the ground swaths of four satellite paths covering the avalanche forecasting region

* *Corresponding author address:*
Markus Eckerstorfer, Norut – Northern Research Institute
P.O.Box 6434, Tromsø Science Park, N-9294 Tromsø, Norway;
tel: +47 926 78 797;
email: markus.eckerstorfer@norut.no

'Tamokdalen' (yellow line) every 12 day. Both monitoring winters started for example with S1A image acquisitions on 31 October (path 095), 2 November (path 131), 4 November (path 160), and 5 November (path 168) followed by a six day break and the start of a new cycle of acquisitions on 12 November (path 095 again).

We downloaded images from the ESA Sentinels Scientific Data Hub (https://scihub.esa.int/dhus) and preprocessed (geocoding and topographic correction) them using our in-house software 'GSAR' (Larsen et al., 2005). The resulting products were single radar backscatter images $\sigma^0(x, y)$ with VH and VV polarization, and separate layover and radar shadow mask files, clipped to the study area and resampled to a spatial resolution of 10x10m.

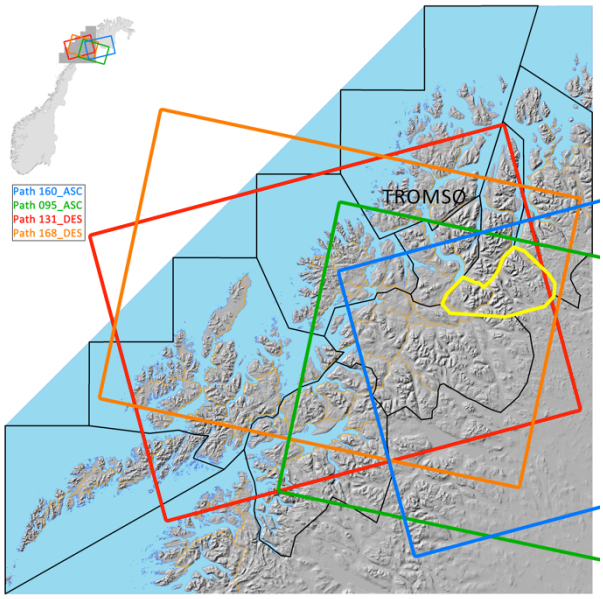

Fig 1: Sentinel-1A image ground swaths of four satellite paths covering the avalanche forecasting region 'Tamokdalen' (yellow line) in Northern Norway. The black lines indicate other avalanche forecasting regions.

2.2 *Manual identification of avalanche debris*

In SAR images, only the debris part of an avalanche is detectable. Backscatter changes in the starting zone are in general not observable. Eckerstorfer and Malnes (2015) concluded that the rough snow surface in avalanche debris is the dominating physical snow parameter that increases backscatter from avalanche debris, relative to the surrounding, undisturbed snowpack. This means that avalanche debris is manually detectable as elongated, tongue-shaped, and downslope extending features, due to its high backscatter and a sharp backscatter contrast to its surrounding. There are obviously other natural phenomena that can cause high backscatter and have an avalanche debris-like shape, such as perennial snow patches, glaciers or debris flow tracks. We have therefore mapped these natural phenomena *a priori* and have applied a slope mask (Bühler et al., 2009) that distinguishes avalanche from non-avalanche terrain. We also used the layover and radar shadow masks to mask out areas with no retrievable backscatter information.

The most important SAR image processing step is the compilation of SAR change detection images (Dsigma) from two single backscatter images of similar geometry and path, with a temporal base line (repeat pass) of minimum 12 days. SAR change detection images show the relative backscatter or the change in backscatter between a 'reference' image (first image in time) and an 'activity' image (image acquired 12 days later). If an avalanche occurred within these 12 days, a change in backscatter (increase) occurred, which was visible in the SAR change detection image. Ideally the temperature and water content of the snow did not change between 'reference' and 'activity' image. If for example the snow cover turned from wet in the 'reference' image to dry in the 'activity' image, this was also shown as an increase in backscatter in the SAR change detection image, which made manual avalanche debris identification difficult.

For the actual manual interpretation of the SAR change detection images, we compiled them into RGB composites where the 'reference' image was set into the red and blue channel and the 'activity' image into the green channel. Thereby an increase in backscatter appeared green, a decrease in backscatter appeared purple, and areas of no temporal backscatter change appeared grey. Avalanche debris therefore appeared as green features that were manually detectable in ArcGIS10. While the delineation of the terminus of identified avalanche debris was in the majority of cases straightforward, due to the sharp backscatter contrast between rough avalanche debris and surrounding undisturbed snow, drawing the perimeter of the uphill part of the avalanche debris bordering the slide path was difficult.

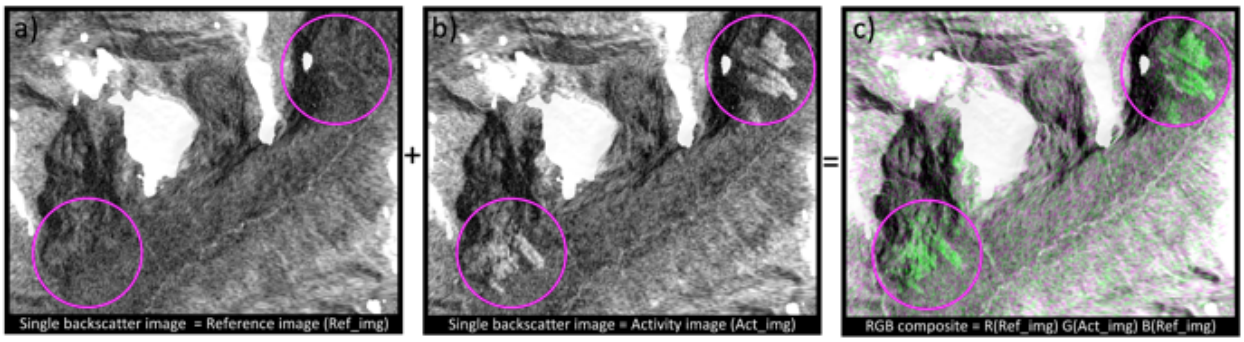

Fig 2: Manual identification of avalanche debris. The change detection method uses a single backscatter image as reference image (Ref_img) (a) without avalanche activity and a subsequent single backscatter image with avalanche activity (Act_img) (b). The result is a RGB composite where avalanche debris appears as green features since the Act_img is set in the green channel.

2.3 Automatic detection of avalanche debris

To make computation efficient, the SAR images are broken into 100 x 100 pixel (1 x 1 km) windows. For each window, a change detection image is formed, in which subsequent masking steps eliminated radar shadow and layover areas, as well as terrain where avalanches are unlikely to occur. Then the percentage of pixels whose backscatter difference value exceeds a specific threshold value (6dB in the case study), indicating the occurrence of avalanche debris, is determined. One % of all pixels in the windows need to have a backscatter change above the threshold value in order to proceed with the data processing, yielding a minimum observable avalanche debris size of 10 pixels (100 x 100m). Feature extraction is then performed on the filtered images using a K-means clustering procedure. This procedure is initialized from a pair of randomly selected pixels and calculates the total dissimilarly between all pixels and the class representatives. We use two classes as we expect a pixel to fall either into the 'avalanche' or 'not avalanche' category. All class 1 'avalanche' pixels are finally transferred onto a DEM and a median filter removes remaining noise.

3. STUDY AREA

The avalanche forecasting region 'Tamokdalen' is located in the county of Troms in northern Norway. Tamokdalen extends over an area of roughly 1600 km^2, encompassing four major valleys and an alpine topography that rises from sea level to 1600m a.s.l. As part of the 23 Norwegian avalanche forecasting regions, daily avalanche bulletins are issued for 'Tamokdalen' and published via www.varsom.no. A field observer is stationed in Tamokdalen, reporting amongst recreation users relevant observations to the crowd sourcing platform www.regObs.no. There is additionally one weather mast located at 1020m a.s.l.

4. RESULTS

4.1 Manual identification of avalanche debris

Here we present manual identification of avalanche debris results from two winters 2014/15 and 2015/16 from 'Tamokdalen' using the four Sentinel-1A satellite paths shown in Fig 1. Our monitoring period each winter stretched between 31 October and 15 June.

During the winter 2014/15, only 52 of 76 S1A images were available, whereas almost a perfect record could be achieved in 2015/16 with 71 out of 76. The reason for missing images is unclear, probably due to the satellite simply not taking an image at times. In both winters, slightly over 1000 features classified as avalanche debris were identified. Subtracting features that were counted two or more times in images of different satellite path, resulted in 736 manually identified avalanche debris in 2014/15 and 796 avalanche debris in 2015/16 respectively (Tbl 1). Highly active avalanche periods debris were 4 – 9 January 2015 with 234 identified avalanche debris and 28 April – 3 May 2016 with 130 identified avalanche debris respectively.

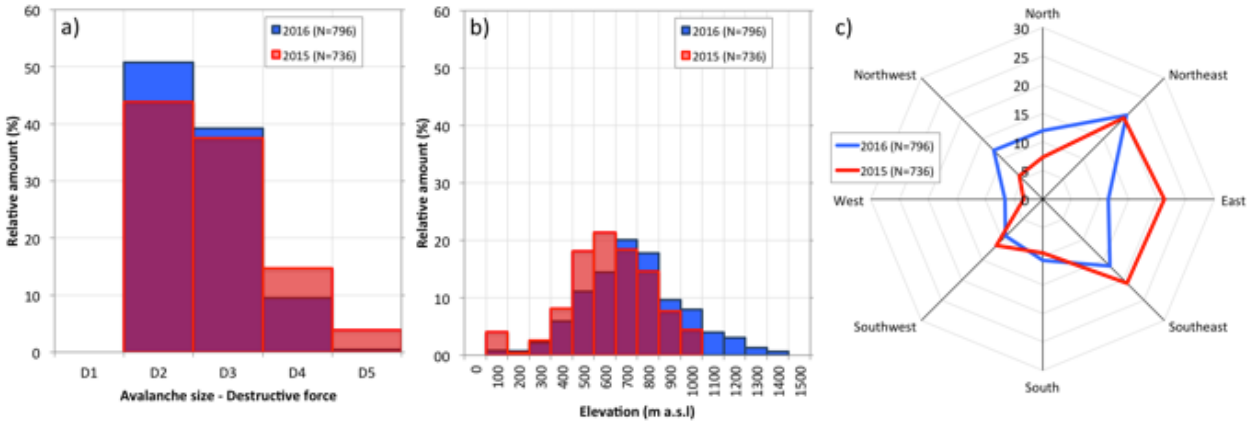

Fig 3: Topographical and morphological parameters of identified avalanche debris during the monitoring winters 2014/15 and 2015/16.

Tbl 1: Summary statistics of satellite paths and SAR images used during the monitoring periods in both winters 2014/15 and 2015/16. The number of manually identified avalanche debris is given for each satellite path.

Satellite paths	*# of images of total images*	*# of identified avalanche debris*
	2014/15	
095_DES	8/19	299
131_ASC	17/19	147
160_ASC	15/19	427
168_DES	17/19	188
Total	52/76	1061 – 325 (doublets) = 736
	2015/16	
095_DES	19/19	243
131_ASC	18/19	164
160_ASC	16/19	355
168_DES	18/19	256
Total	71/76	1018 – 222 (doublets) = 796

4.2 *Topographical and morphological parameters of manually identified avalanche debris*

In both winters, D2 and D3 avalanche sizes dominated, with some larger avalanche debris also identified (Fig 3a). The complete lack of D1 avalanche debris is due to the spatial resolution of S1A images, which does not allow for identification of small avalanche debris. There are larger differences in the elevation distribution of avalanche debris between both winters (Fig 3b). Avalanche debris in 2014/15 occurred in general at lower elevations with than in 2015/16 with no avalanche debris identified above 1000 m a.s.l. The aspect distribution of identified avalanche debris again yields comparable results between both winters, with higher frequency of identified avalanche debris in Northeast to southeast sectors (Fig 3c).

Merging the datasets of identified avalanche activity from both winter seasons' results in a map of avalanche paths that are frequented between one and ten times (Fig 4). Avalanche debris was identified in 680 unique avalanche paths of which 404 paths were frequented by an avalanche once. There are, however fourteen paths that released seven and more avalanches.

4.3 *Validation of manual avalanche debris identification*

Manual identification of avalanche debris is subject to user interpretation, especially the delineation of features identified as avalanche debris. Particularly the delineation uphill part of an avalanche debris is in many cases difficult, as a clear backscatter contrast between avalanche debris and surrounding undisturbed snow often does not exist, as opposed to the area of the debris terminus. Thus, different observers would likely delineate identified avalanche debris slightly different, and aggregate multiple adjacent avalanche debris differently. Due to the change detection method, in combination with a slope mask, there is, however, only a very small chance that a downslope extending, tongue-shaped feature appearing in a change detection image is anything else than avalanche debris. Especially if multiple overlapping satellite paths with consecutive acquisition dates are used and

the avalanche debris appears in all of them repeatedly.

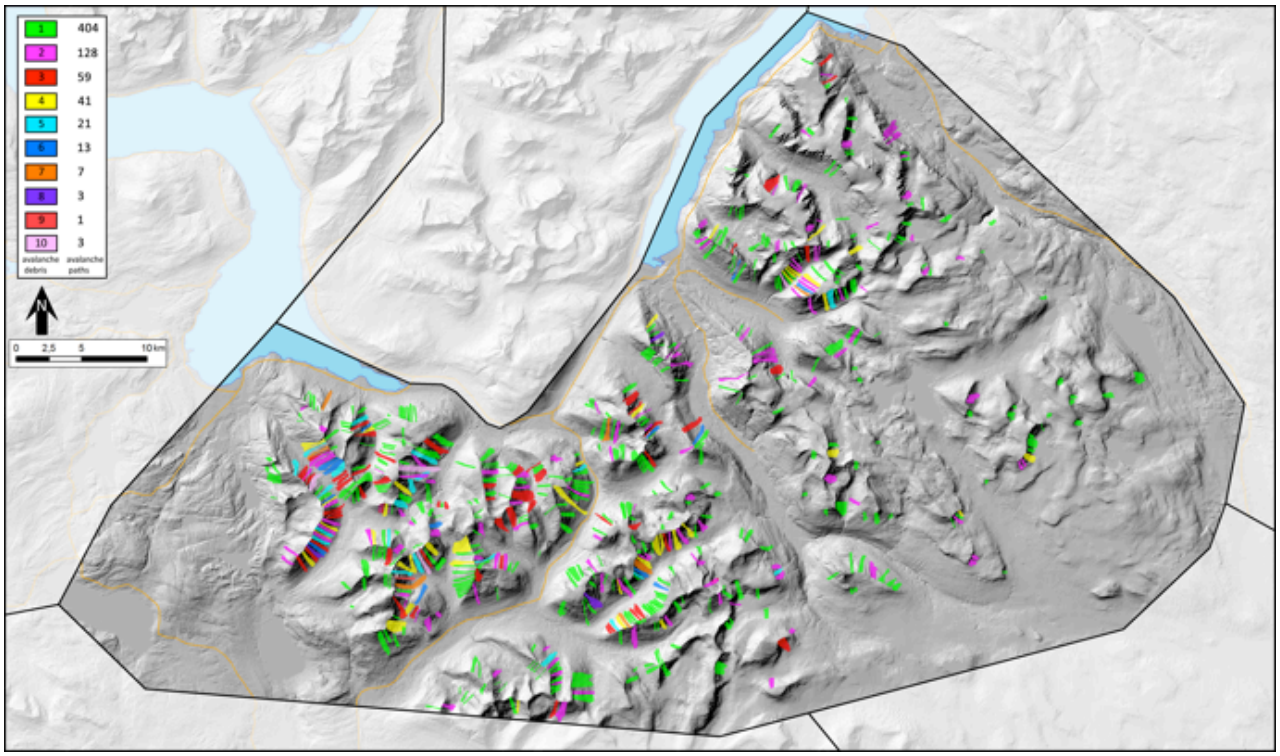

Fig 4: Inventory of the frequency of identified avalanche debris in avalanche paths from both monitored winters 2014/15 and 2015/16 in 'Tamokdalen'.

4.4 Automatic detection of avalanche debris

With the launch of Sentinel-1B, the twin satellite to S1A, we will be able to fill in the six days data gaps we currently have, thus acquiring a SAR image every second day. This data availability offers the possibility to collect a complete, consistent avalanche activity database for an entire winter in 'Tamokdalen'. Such a data set could be used to compare with triggering meteorological factors, as well as for validation of the given regional avalanche danger level. However, manual identification would be too time consuming, thus we have developed an automatic avalanche debris detection algorithm.

To show the performance of the algorithm, we present a comparison of manual identified and automatically detected avalanche debris, exemplified by one case study, zoomed in on an area of high avalanche activity in 'Tamokdalen' (Fig 5). Of 70 manually identified avalanche debris, 40 (57%) were also captured by the algorithm, using a threshold of 6dB. In terms of numbers of pixels, 62 % were identified both manually and automatically at the same location. In general, location and morphology of manually and automatically detected avalanche debris agree better than the exact shape.

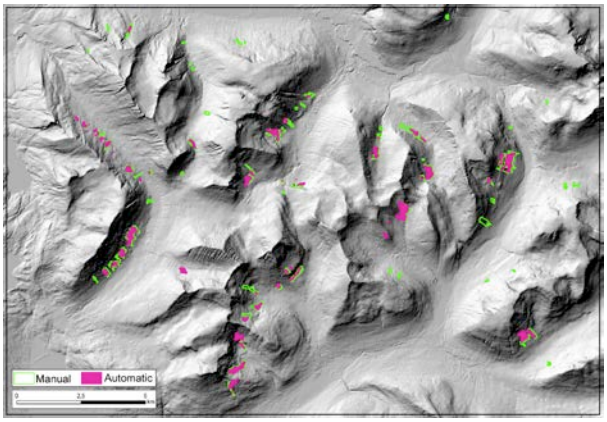

Fig 5: Comparison between manual identified (green outlines) and automatically detected avalanche debris (pink areas) on 9 January 2015, using path 168_DES.

It is clear that the threshold applied, which determines if a pixel is classified as 'avalanche' or 'not avalanche has significant influence on the classification outcome. A lower threshold allows the algorithm to achieve a higher fraction of correctly classified pixels, however at the expense of a high fraction of 'false positive' pixels (Tbl 2). If the threshold is increased, the algorithm misses a greater fraction of the manually identified avalanche pixels, however, the false positive pixels are reduced.

Tbl 2: Percentage of correctly classified, misclassified (commission error) and missed pixels (omission error) by the automatic avalanche debris detection algorithm compared to manually identified avalanche debris on 9 January 2015.

Threshold (dB)	*% correctly classified*	*Commission error*	*Omission error*
5.0	67.5	87.3	32.5
6.0	62.3	53.9	37.7
7.0	54.8	20.8	45.2

The first results of the automatic avalanche debris detection are promising, however, there are a number of challenges still to be solved. The algorithm is highly dependent on both images used for change detection having similar snow conditions (either dry – dry or wet – wet). Snow-covered trees can be also falsely detected as avalanche debris by the algorithm. The comparison between manually identified and automatically detected avalanche debris has also its pitfalls, mostly since we do not have sufficient field validation data. There is also the problem of manually delineating avalanche debris (as stated above) which has influence on the pixel to pixel comparison between manually and automatically obtained detections.

5. CONCLUSION

Sentinel-1A is a radar satellite that provides high resolution SAR data with a large ground swath, covering every location on Earth every 12 days. As the satellite is in a polar orbit, high latitudes are covered more frequently as satellite paths merge. We used S1A images to both manually identify and automatically detect avalanche debris in the Norwegian avalanche forecasting region 'Tamokdalen', located southeast of Tromsø. For detection, we used a change detection method that produces images where backscatter change over time becomes visible. Avalanche debris exhibits an increase in backscatter and become therefore detectable. Using manual identification of avalanche debris, we were able to collect datasets of avalanche activity during two winters, from which we could deduce topographical and morphological parameters of avalanche activity as well as the most prone avalanche paths. In an operational context, an automatic detection algorithm is needed which we are currently developing and showing its performance in a case study. Using automatic detection and images from the recently launched Sentinel-1B satellite, which cuts worldwide revisit time in half to six days, will allow for complete, reliable and consistent operational avalanche activity monitoring in any given avalanche forecasting region.

ACKNOWLEDGEMENTS

This research was conducted within the SeFaS project, financed by RDA Troms, as well as the ESA Living Planet Fellowship (AVISENT).

REFERENCES

Bühler, Y., Hüni, A., Christen, M., Meister, R. and Kellenberger, T., 2009. Automated detection and mapping of avalanche deposits using airborne optical remote sensing data. Cold Regions Science and Technology, 57(2–3): 99-106.doi: 10.1016/j.coldregions.2009.02.007

Deems, J.S., Painter, T.H. and Finnegan, D.C., 2013. Lidar measurement of snow depth: a review. Journal of Glaciology, 59: 467-479.doi:10.3189/2013JoG12J154

Eckerstorfer, M., Bühler, Y., Frauenfelder, R. and Malnes, E., 2016. Remote sensing of snow avalanches: recent advances, potential, and limitations. Cold Regions Science and Technology, 121: 126-140.doi:10.1016/j.coldregions.2015.11.001

Eckerstorfer, M. and Malnes, E., 2015. Manual detection of snow avalanche debris using high-resolution Radarsat-2 SAR images. Cold Regions Science and Technology, 120: 205-218.

Larsen, Y., Engen, G., Lauknes, T.R., Malnes, E. and Høgda, K.A., 2005. A generic differential interferometric SAR processing system, with applications to land subsidence and snow-water equivalent retrieval. In: E. ESRIN (Editor), Fringe ATSR Workshop 2005, Frascati, Italy, pp. 6.

Prokop, A., Schön, P., Wirbel, A. and Jungmayr, M., 2014. Monitoring avalanche activity using distributed acoustic fiber optic sensing, Proceedings of the International Snow Science Workshop, 2014, Banff, Alberta, Canada, pp. 129-133.

van Herwijnen, A., Berthod, N., Simenhois, R. and Mitterer, C., 2013. Using time-lapse photography in avalanche research, Proceedings of the International Snow Science Workshop, 2013, Grenoble, France, pp. 950-954.

van Herwijnen, A. and Schweizer, J., 2011. Monitoring avalanche activity using a seismic sensor. Cold Regions Science and Technology, 69(2-3): 165-176.doi: 10.1016/j.coldregions.2011.06.008